Research Article

Nur Nida Syamimi Subri, Siti Nurul Ain Md. Jamil*, Peter A. G. Cormack, Luqman Chuah Abdullah, Sazlinda Kamaruzaman, and Abel A. Adeyi

The synthesis and characterisation of porous and monodisperse, chemically modified hypercrosslinked poly (acrylonitrile)-based terpolymer as a sorbent for the adsorption of acidic pharmaceuticals

https://doi.org/10.1515/epoly-2020-0037
received January 23, 2020; accepted March 20, 2020

Abstract: The synthesis and characterization of porous poly(acrylonitrile(AN)-*co*-divinylbenzene-80 (DVB-80)-*co*-vinylbenzylchloride (VBC)) polymers with high specific surface areas and weak anion-exchange character have been successfully researched. The hypercrosslinked (HXL) microspheres were chemically modified with 1,2-ethylenediamine (EDA) to enhance the adsorption selectivity of the HXL materials. The zeta potential of EDA-modified HXL poly(AN-*co*-DVB-80-*co*-VBC) revealed that the surface of the modified terpolymer was positively charged. The FT-IR spectra of the chemically modified hypercrosslinked poly(AN-*co*-DVB-80-*co*-VBC) showed that the nitrile groups derived from the AN unit were utilised by the presence of diamine groups. The BET-specific surface areas of the EDA-modified hypercrosslinked poly(AN-*co*-DVB-80-*co*-VBC) was 503 $m^2 g^{-1}$; meanwhile, the specific surface area of the HXL terpolymer was 983 $m^2 g^{-1}$. The adsorption isotherm data were well fitted by both the Langmuir and Freundlich models, whereas the adsorption kinetics followed the pseudo-second-order kinetic model. This study confirms that the EDA-modified hypercrosslinked poly(AN-*co*-DVB-80-*co*-VBC) terpolymer is a potential adsorbent for the adsorption of acidic pharmaceuticals.

Keywords: chemical modification, hypercrosslinked terpolymer, monodispersity, pharmaceuticals, selectivity

1 Introduction

The presence of a pharmaceutically active compound in surface and groundwater is a matter of great concern as they are used as a resource for the production of potable water. Pharmaceutical residues have been reported as potential contaminants to aquatic species and seafood consumers (1). Pharmaceuticals can be introduced into the environment through various routes, primarily through wastewater treatment plants (WWTPs) after the manufacturing of medicine (2). The continuous release of pharmaceuticals in the sewage system will be further degraded or removed; however, some residues will remain and be present in very small concentrations in WWTPs, hospitals' influent and effluent, and drinking water (3,4). Caffeine, levonorgestrel, and diclofenac-Na have been detected at concentrations of 4,005, 447, and 2,008 ng L^{-1}, respectively, in a sewage treatment plant in Malaysia (5). Praveena et al. investigated the occurrence of nine pharmaceuticals in three main rivers (Liu, Gombak, and Selangor) in Malaysia and exposed the highest pharmaceutical concentrations in the Gombak river (ciprofloxacin, 299 ng L^{-1}) (6). Large production of pharmaceuticals, an increase in drug consumption, and the type of wastewater treatment technology are possible reasons that have led to the pharmaceutical occurrence in the aquatic environment (7).

Among the wide variety of pharmaceuticals, diclofenac, mefenamic acid, and metronidazole are the most common acidic drugs detected in the water samples. Diclofenac (DCF; $pK_a = 4.15$) and mefenamic acid (MA; $pK_a = 4.20$), a group of

* **Corresponding author: Siti Nurul Ain Md. Jamil,** Department of Chemistry, Faculty of Science, Universiti Putra Malaysia, 43400 Serdang, Selangor D.E., Malaysia; Centre of Foundation Studies for Agricultural Science, Universiti Putra Malaysia, 43400 UPM Serdang, Selangor, Malaysia, e-mail: ctnurulain@upm.edu.my
Nur Nida Syamimi Subri, Sazlinda Kamaruzaman: Department of Chemistry, Faculty of Science, Universiti Putra Malaysia, 43400 Serdang, Selangor D.E., Malaysia
Peter A. G. Cormack: WestCHEM, Department of Pure and Applied Chemistry, University of Strathclyde, Thomas Graham Building, 295 Cathedral Street, Glasgow G1 1XL, Scotland, UK
Luqman Chuah Abdullah: Department of Chemical and Environmental Engineering, Faculty of Engineering, Universiti Putra Malaysia, 43400 Serdang, Selangor D.E., Malaysia
Abel A. Adeyi: Department of Chemical and Petroleum Engineering, College of Engineering, Afe Babalola University Ado-Ekiti, ABUAD, KM. 8.5, Afe Babalola Way, P.M.B. 5454, Ado-Ekiti 360211, Nigeria

non-steroidal anti-inflammatory drug (NSAID), are extensively studied pharmaceuticals due to their potentially toxic effects and low biodegradability, resulting in low elimination rates in WWTPs (8,9). Metronidazole (MNZ; pK_a = 2.62), an anti-inflammatory and antibacterial agent, is one of the most heavily used antibiotics, which has a very high solubility in water and is expected to be highly mobile in aqueous systems (10).

The removal of pharmaceuticals from wastewater can be performed by the adsorption process with particular adsorbents. The adsorption characteristics of a particular adsorbent largely depend on its specific surface area, selectivity, and the presence of accessible active functional groups (11). The silica-based materials were first chemically modified with C_8, C_{18}, phenyl, CN, or NH_2 groups as sorbents for solid-phase extraction (SPE) processes (12). However, these silica-based sorbents presented several disadvantages, including instability at extreme pH and low recovery in the extraction of polar compounds (13). Thus, porous polymeric sorbents were shown to be effective due to their monodispersity, easy chemical modification, and extreme stability across the entire pH range (14,15). This is especially true for adsorbent based on the cross-linked (or hypercrosslinked [HXL]) polymers that became as d-SPE sorbents since they had high porosity (above 1,000 $m^2 g^{-1}$), tunable chemistry and a high micropore content (13,16). Huang et al. synthesised a series of naphthol-modified hypercross-linked resin from microporous poly(styrene-*co*-divinylbenzene), which determined different adsorption selectivity toward salicylic acid due to their different surface area and pore structure (17). It was also reported that the hypercrosslinking of polydivinylbenzene (poly (DVB)) via Friedel Crafts reaction had successfully increased the porosity of poly(DVB) (~600 $m^2 g^{-1}$) up to 2,000 $m^2 g^{-1}$ (18). However, HXL sorbents are normally available as polydisperse with a large particle size (50–200 μm) due to its preparation via the dispersion polymerisation method. The same case was reported by Subri et al., where the hypercrosslinking of poly(acrylonitrile(AN)-*co*-divinylbenzene-80 (DVB-80)-*co*-vinyl benzyl chloride (VBC)) had successfully obtained high specific surface areas up to 1,080 $m^2 g^{-1}$ with polydisperse polymer microspheres, via synthesis from the Friedel–Crafts reaction (19). Hence, the heterogeneity in particle size distribution had led to inefficient packing of the sorbent and poor interaction with the solutes (20).

In addition, the polymeric sorbents such as highly selective ion-imprinted polymers (IIP) also have been widely employed as SPE packing materials to provide better affinity and selectivity for the removal of metal particles. Taheri and his coworker successfully synthesised a novel magnetic ion-imprinted polymer (MIIP) using Fe_3O_4@SiO_2@TiO_2 nanoparticles, with methacrylic acid (MAA) and ethylene glycol dimethylacrylate (EGDMA) as the functional monomer and crosslinker, respectively, via the sol–gel polymerization method for the removal of silver ions. The increased selectivity of the nanostructured MIIP particles as a sorbent was shown a greater adsorption capacity (which is 62.5 mg g^{-1}) toward Ag(I) ions compared to other cations (21). Another selective extraction of metal ion (cobalt(II) ion) from environmental samples was carried out by the prepared magnetic Fe_3O_4@-SiO_2@TiO_2-IIP nanoparticles sorbent that had been functionalised with –NH groups, using the sol–gel surface imprinting technique. The results showed that the particles of Fe_3O_4@SiO_2-IIP were uniform in size, showing an average diameter of 140 nm, which plays the most important criteria for the application of SPE column packing (22). High selectivity and high adsorption capacities, along with lower detection limits, give better advantages to the IIP technology to be exploited as one of the selective adsorbents in the SPE applications (23).

Another approach to produce a polymeric material with higher capacity, sensitivity, and selectivity is via a chemical modification, which tunes the functionality of the HXL materials toward the extraction of the polar compounds. The presence of various types of polar and active functional groups in the modified sorbent is expected to provide ion-exchange characteristics to adsorb polar, non-polar, neutral, and cationic compounds simultaneously from the aqueous media (15). The introduction of polar groups can enhance the hydrophilicity of the materials (24). The hydrophilic sorbents can be prepared either by copolymerization of the functional monomers or by chemically modifying the hydrophobic polymers with polar moieties, before or after the hypercrosslinking reaction. Fontanals et al. carried out the post-hypercrosslinking chemical modification on poly(DVB80-VBC) copolymer, by modifying two amine moieties, 1,2-ethylenediamine (EDA) and piperazine, that took place on the residual chloromethyl groups from the VBC units in the copolymer. As a consequence, the porosity of the chemically modified HXL copolymers was retained throughout the chemical modification process with the presence of weak anion-exchange (WAX) character (25). Other post-functionalised HXL resins were prepared from either acetyl sulfate or lauryl sulfate, giving rise to the synthesis of hypercrosslinked strong cation-exchange (HXL-SCX) material due to the presence of sulfonic acid groups. It was found that 50% of lauryl sulfate–modified HXL-SCX copolymer displayed the highest specific surface areas (1,370 $m^2 g^{-1}$) although the sulphonate group was only developed within the benzene ring of the methylene bridge (upon hypercrosslinking reaction) (26). Similar HXL SCX materials were reported by

synthesising VBC-EGDMA in different ratios, and then, the HXL-NAD particles were sulfonated using sulphuric acid. After the sulphonation reaction, the specific surface areas increased from 300 up to 1,000 $m^2 g^{-1}$ (27). For the pre-modification reaction, the VBC-DVB precursors (which were obtained via precipitation polymerisation) were modified first with 5% and 10% dimethylbutylamine (DMBA) to introduce the strong anion-exchange (SAX) character. The DMBA-modified VBC-DVB particles were then hypercrosslinked via Friedel–Crafts reaction, and it was discovered that the amination was less efficient subsequent to hypercrosslinking due to the bulky nature of the tertiary amine, which restricted the amine's access to the free chloromethyl groups (28).

A previous work reported by Subri and coworkers described the precipitation polymerisation of poly(AN-*co*-DVB-80-*co*-VBC) terpolymers in the form of porous polymer microspheres, which then hypercrosslinked, via Friedel–Crafts reaction with iron(III) chloride, $FeCl_3$ as a catalyst, to provide a significant lift in specific surface areas of polymers (as shown in Scheme 1). It was found that hypercrosslinked poly(AN-*co*-DVB-80-*co*-VBC) was successfully utilized for the capture of diclofenac polar compound with the maximum adsorption up to 95% (303 mg g^{-1} of adsorption capacity) (29). These highly porous polymers with polar character arising from the inclusion of AN residues are attractive candidates as potential sorbents during SPE.

However, there has been little discussion about the utilisation of acrylonitrile-based polymer as an adsorbent for the adsorption of pharmaceutical residues. Thus, in this present study, the cyano groups in the HXL poly(AN-*co*-DVB-80-*co*-VBC) terpolymer were chemically modified with ethylenediamine (EDA) to develop weak anion-exchange (WAX) characters in the sorbent system by converting the nitrile functional groups into diamine moieties to enhance the selectivity of the sorbent. The development of the WAX character is expected to offer improved performance of modified acrylonitrile-based hypercrosslinked precursor resin toward pharmaceuticals with various ionic charges.

To date, the preparation of synergistic sorbent materials (chemically modified hypercrosslinked poly(acrylonitrile (AN)-*co*-divinylbenzene-80 (DVB-80)-*co*-vinyl benzyl chloride (VBC)) in the form of monodisperse microspheres associated with good selectivity and capacity toward polar compounds has not been reported elsewhere (Scheme 2).

2 Experimental

2.1 Materials and chemicals

The reagents used for the polymer synthesis were acrylonitrile (AN; ≥99% grade, Merck, Netherlands), divinylbenzene-80 (DVB-80; 80% grade, Sigma-Aldrich, Dorset, UK), and 4-vinyl benzyl chloride (VBC; 90% grade, Sigma-Aldrich, Dorset, UK). AN, DVB, and VBC were purified by passing the monomers,

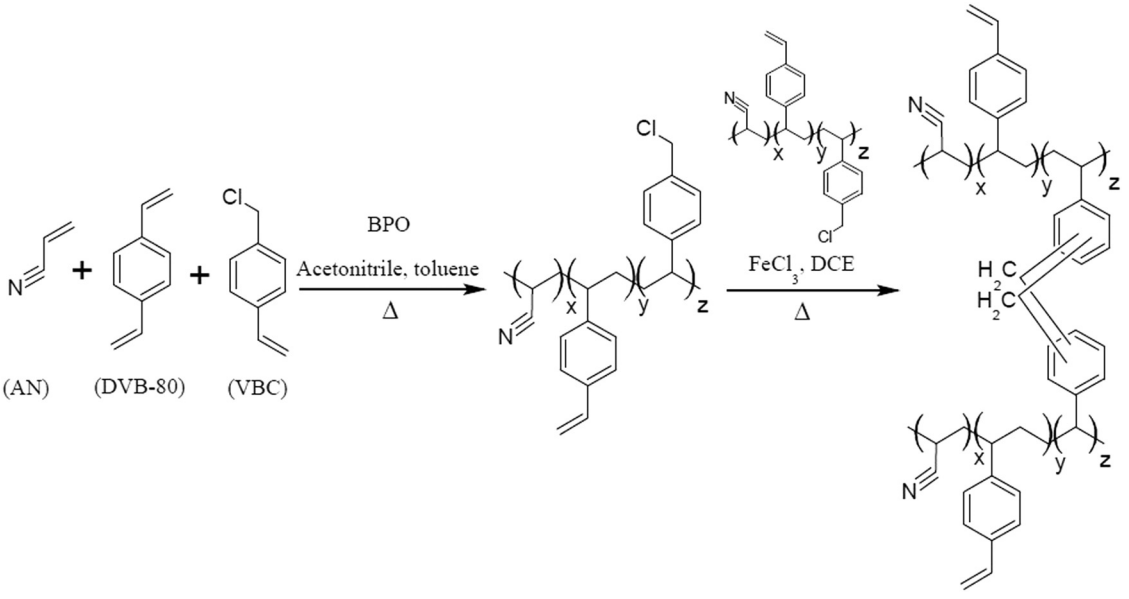

Scheme 1: The schematic of hypercrosslinking reaction of poly(AN-*co*-DVB-80-*co*-VBC) terpolymer, synthesised by the precipitation polymerisation method.

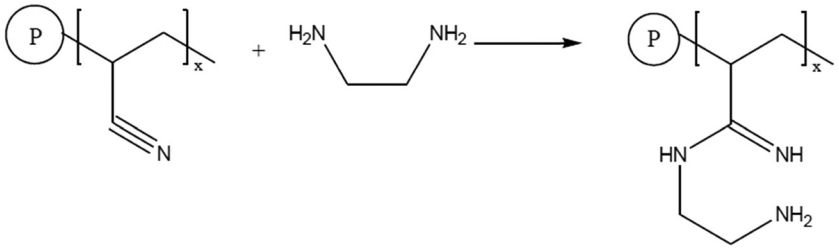

Scheme 2: Scheme of the synthesis of EDA-modified HXL poly(AN-*co*-DVB-80-*co*-VBC). *P is HXL poly(AN-*co*-DVB-80-*co*-VBC) and the nitrile group is shown due to the chemical modification on the nitrile groups.

respectively, through a neutral alumina column. The benzoyl peroxide (BPO) that was used as an initiator was supplied by Sigma-Aldrich (Dorset, UK) and purified by recrystallization from acetone (≥99% grade; Sigma-Aldrich, UK). Acetonitrile (HPLC grade), toluene (≥99% grade), and methanol (≥99% grade) were supplied by Sigma-Aldrich (Dorset, UK). 1,2-Dichloroethane (DCE) (>99% grade) (Sigma-Aldrich) and ferric chloride ($FeCl_3$; Fisher, US) were used as reagents in hypercrosslinking reactions. Ethylenediamine (EDA; >99% grade; R&M Chemicals, UK) was used to chemically modify the hypercrosslinked resin. All other reagents were used as received.

2.2 Precipitation polymerisation of poly (AN-*co*-DVB-80-*co*-VBC)

DVB-80 (0.60 mol), VBC (0.05 mol), and AN (0.35 mol) were added to a Nalgene® plastic bottle. BPO and a mixture of acetonitrile and toluene were then added to the Nalgene® bottle. The bottle was sealed lightly with parafilm and placed in an ultrasonic bath for 10 min. Then, the bottle was placed on an ice bath and deoxygenated by sparging it with nitrogen gas for 30 min. After resealing, the bottle was placed on a low-profile roller and rotated slowly, spinning about its long axis at 10 rpm. The temperature of the incubator was increased from ambient to 60°C over a period of approximately 2 h. The polymerisation was allowed to occur for 94 h after the incubator reached 60°C. After the 96 h period, the milky suspension of the polymer particles was then filtered using a 0.20 µm nylon membrane and washed with 20.00 mL of respective acetonitrile, toluene, methanol, and acetone. After washing, the polymer sample was dried in a vacuum oven at 40°C overnight (29).

2.3 Hypercrosslinking reactions

The terpolymer particles (1.00 g) and 30.00 mL of DCE were placed in a round-bottomed flask, and the mixture was left under nitrogen for 1 h to swell the beads. Then, $FeCl_3$ that was suspended in DCE was added. The mixture was heated rapidly to 80°C and kept at this temperature for 18 h. The hypercrosslinked particles were filtered, washed with methanol, and then washed several times with aqueous HNO_3 (pH 1). Then, the particles were extracted overnight with acetone in a Soxhlet extractor and washed again with methanol and diethyl ether before overnight drying to constant mass in a vacuum oven at 40°C (29).

2.4 Diamine modification of hypercrosslinked poly(AN-*co*-DVB-80-*co*-VBC)

The hypercrosslinked resin and DCE were placed in a round-bottomed flask, and the mixture was left under nitrogen for 4 h to wet the beads. Then, ethylenediamine (EDA) was added to the solution. The mixture was heated rapidly to 90°C and kept at this temperature for 24 h. The particles were filtered and washed with toluene, methanol, and several times with aqueous 5% (w/v) $NaHCO_3$ (pH 9) and water. The resin was dried overnight in a vacuum oven at 40°C.

2.5 Characterisations

2.5.1 Fourier transform infra-red spectroscopy

Fourier transform infrared (FT-IR) spectra were recorded using a spectrum BX Perkin Elmer (United States) with Universal Attenuated Total Reflectance (UATR) technique to identify the presence of functional groups in the polymers. The infrared spectra of the samples were measured in the range between 280 and 4,000 cm^{-1} at 25°C.

2.5.2 Scanning electron microscopy

Scanning electron microscopy (SEM; JEOL JSM 6360LA, Japan) was used to observe the morphology of the polymer

particles produced. A steel stub was coated with conductive copper using double-sided adhesive tape. A thin layer of the sample was then deposited onto the coated steel stub. The platinum coating of the immobilised sample was carried out for 8 min. A coated sample was then placed inside the SEM chamber, and a vacuum was applied. Micrographs were acquired at accelerating voltages of 10.0 kV or 25.0 kV. The microsphere diameters and particle size distributions were calculated using ImageJ software from the SEM image analysis of 100 individual particles.

2.5.3 Energy dispersive X-ray (EDX) spectroscopy

The amount of chlorine present in the polymeric particles was determined using a Thermo Fisher Scientific (USA) Noran System 7 X-ray Microanalysis System in conjunction with a SEM. The X-ray intensity was measured relative to the lateral position of the sample by using elemental mapping. Variations in X-ray intensity at any characteristic energy value indicate the relative concentration for the element across the surface.

2.5.4 Elemental microanalysis

Carbon, hydrogen, and nitrogen contents were determined using a PerkinElmer 628 Series instrument at the Material Characterisation Laboratory at the Faculty of Engineering, UPM. The samples were wrapped in tin foil and combusted at 1,800°C in pure oxygen. The combustion products were catalysed, and the interferences were removed before being swept into a detection zone where each element was separated and eluted as CO_2, H_2O, and NO_2. The signals were then converted to a percentage of elements.

2.5.5 Zeta potential

Zeta potential was measured using a Zetasizer Nano Series (Malvern Panalytical Limited, UK) to provide information about surface charge(s) of synthesised, hypercrosslinked, and chemically modified hypercrosslinked terpolymers.

2.5.6 Nitrogen sorption analysis

The specific surface areas, specific pore volumes, and mean pore sizes of polymer microspheres were measured using a nitrogen sorption porosimeter, model Micrometrics ASAP 2010 (USA) surface area analyser. Samples were degassed overnight under vacuum at 100°C and then analysed using nitrogen sorption carried out at 77 K. The relative pressure and the quantity of gas adsorbed were measured to give an adsorption isotherm. The samples were analysed with computer control Module ASAP 2010 Version 2.00, and the surface area was then calculated using the Langmuir and BET (Brunauer, Emmet, and Teller) equations.

2.6 Adsorption experiments

The adsorption of diclofenac (DCF) onto EDA-modified HXL terpolymer was carried out using batch experiments by adding 10.00 mg of adsorbent into 20.00 mL of diclofenac solutions. The solution was left to equilibrate overnight before analysis. The solution was then centrifuged for 10 min at 4,000 rpm at a room temperature of 25°C. 3 mL aliquot of the supernatant was taken out and filtered in 0.200 µm Millipore filter syringe and then analysed by using PerkinElmer (United States) Lambda 35 UV-Vis spectrometer in the range of 200–400 nm of absorbance. The same procedures were repeated for the adsorption of mefenamic acid (MA) and metronidazole (MNZ). The percentage removal of pharmaceuticals is expressed in Eq. 1:

$$q_e = \frac{C_o - C_e}{C_o} \times 100 \quad (1)$$

where q_e (%) is the percentage of adsorbate being adsorbed by the adsorbent at equilibrium with initial concentration C_o and the equilibrium adsorbate concentration in solution C_e (mg L^{-1}).

2.7 Equilibrium isotherms

The adsorption isotherms were determined by varying the initial concentration of diclofenac, mefenamic acid, and metronidazole (20–260 mg L^{-1}) with 0.01 g of EDA-modified HXL terpolymer adsorbent. The adsorption capacity at equilibrium was calculated by using Eq. 2:

$$q_e = \frac{C_o - C_e}{m} \times V \quad (2)$$

where q_e (mg g^{-1}) is the amount of adsorbate adsorbed on per gram of adsorbent at equilibrium. C_o and C_e represent the initial and equilibrium concentration in

solution (mg L^{-1}), respectively. m (g) is the amount of adsorbent used, and V (L) is the volume of the solution. The obtained data were further analysed by plotting a graph of $1/q_e$ versus $1/C_e$ for the Langmuir isotherm model and of $\log q_e$ versus $\log C_e$ for the Freundlich isotherm model.

2.8 Adsorption kinetic study

The adsorption kinetics study was examined by varying the contact time (2, 4, 6, 8, and 10 min) with 10.00 mg of EDA-modified HXL terpolymer as adsorbent. The amount of drugs adsorbed by the adsorbent at time t was calculated by using Eq. 3:

$$q_t = \frac{C_o - C_t}{m} \times V \quad (3)$$

where q_t (mg g^{-1}) is the amount of adsorbate adsorbed on per gram of the adsorbent at time t. C_o and C_t represent the initial concentration and adsorbate concentration at time t in solution (mg L^{-1}), respectively. m (g) refers to the amount of adsorbent, and V (L) represents the volume of the solution. The collected data were then analysed using the kinetic model, which includes the Lagergren pseudo-first-order and pseudo-second-order models to investigate the adsorption mechanism.

3 Results and discussion

3.1 Fourier transform infrared analysis

Figure 1a and b show the FT-IR spectra of the poly(AN-*co*-DVB-80-*co*-VBC) terpolymers before and after the hypercrosslinking reactions, respectively. Both FT-IR spectra showed a strong absorption band at ~2,244 cm^{-1}, which corresponded to the stretching vibration of the nitrile groups, thereby confirming the AN incorporation. The absorption band at ~1,270 cm^{-1}, which was assigned to the chloromethyl groups, was presented in poly(AN-*co*-DVB-80-*co*-VBC) FT-IR spectrum (Figure 1a); however, this band almost disappeared in the HXL poly(AN-*co*-DVB-80-*co*-VBC) spectrum (Figure 1b) following hypercrosslinking, which was the result of the consumption of chloromethyl groups. This confirmed that the hypercrosslinking reaction that involved nucleophilic substitution in the Friedel–Crafts alkylation reaction was successfully carried out (29).

Figure 1c shows the FT-IR spectrum of hypercrosslinked poly(AN-*co*-DVB-80-*co*-VBC) that was chemically modified with ethylenediamine (EDA). After diamine modification, some of the functional group(s) in the HXL poly(AN-*co*-DVB-80-*co*-VBC) disappeared and the formation of new functional groups was observed. The absorption band assigned to the CN stretching vibration at ~2,244 cm^{-1} was diminished in the spectrum of EDA-modified HXL terpolymer,

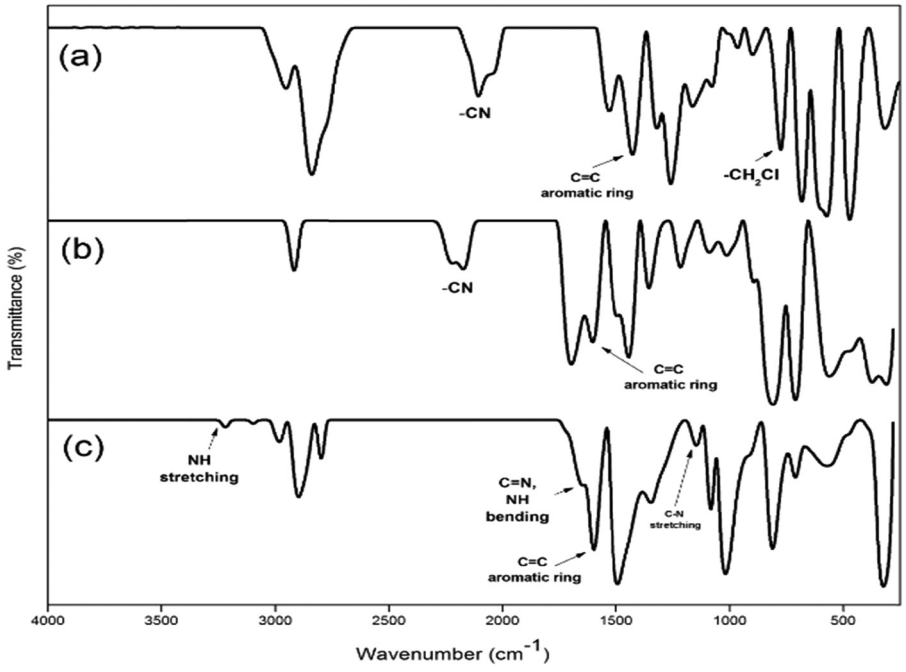

Figure 1: FT-IR spectra of (a) P1, (b) HXL P1, and (c) EDA-HXL P1, respectively.

indicating that the nitrile group was successfully converted into diamine moieties. This can be proved by the presence of a new peak at 3,328 cm^{-1}, which corresponded to the $-NH_2$ stretching vibration. The FT-IR spectrum also showed a new absorption band at 1,648 cm^{-1} due to the overlapping of NH and C=N bending vibrations. The appearance of a peak at 1,598 cm^{-1} was related to the C=C stretching vibration from aromatic rings. This affirmed that the weak anion exchange character was developed via the incorporation of diamine active pendant groups in the modified-hypercrosslinked terpolymer surface.

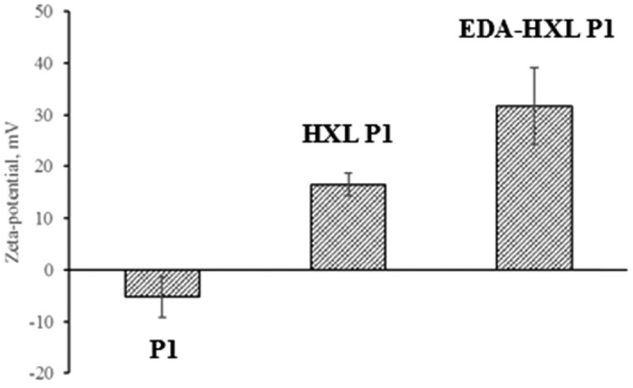

Figure 2: Zeta-potential of P1, HXL P1, and EDA-HXL P1 terpolymers, respectively.

3.2 Elemental microanalysis

Elemental microanalysis was carried out to estimate the composition of the chemically modified hypercrosslinked polymers isolated from the precipitation polymerisation. The C, H, N, and Cl contents of poly(AN-*co*-DVB-80-*co*-VBC) and HXL poly(AN-*co*-DVB-80-*co*-VBC) terpolymers before and after chemical modification with EDA are presented in Table 1. In the case of P1 and HXL P1, the N contents were 3.8% and 3.1%, respectively, which were in agreement with their expected N contents (P1 [4.7%] and HXL P1 [3.5%]). Meanwhile, the Cl contents decreased from 1.0% to 0.6% as the chloromethyl groups derived from VBC were consumed by the Friedel–Crafts reactions. After the amination of the hypercrosslinked terpolymers, the percentage of C contents had reduced to 65.1%; meanwhile, the percentage of N contents increased to 20% (EDA-HXL P1). This was due to the presence of a secondary amino group from the ethylenediamine found during the chemical modification of hypercrosslinked poly(AN-*co*-DVB-80-*co*-VBC) terpolymers.

3.3 Zeta potential measurements

Zeta potentials of poly(AN-*co*-DVB-80-*co*-VBC) (P1), hypercrosslinked poly(AN-*co*-DVB-80-*co*-VBC) (HXL P1), and diamine-modified hypercrosslinked poly(AN-*co*-DVB-80-*co*-VBC) (EDA-HXL P1) terpolymer samples are shown in Figure 2. The zeta potential of EDA-HXL P1 (31.7 mV) was the highest, indicating the development of weak anion-exchange character as a result of the chemical modification of diamine functional groups that provided a net positive surface charge when suspended in water. The cationic group of EDA-HXL P1 promoted ion-exchange interactions with anionic compounds (deprotonated acidic compound) (pH > pK_a) (30). Deprotonation improved the hydrophilicity of the acidic compounds that led to greater sorption with more hydrophobic regions of EDA-HXL P1 (31). The increase in the zeta potential confirmed the availability of more positively charged amine groups at the edges of the modified hypercrosslinked terpolymer surface compared to HXL P1 (16.5 mV). The zeta potential value of the aqueous dispersion of P1 was negative (–5.3 mV). These results implied that positively charged EDA-HXL P1 terpolymer surface enhanced the selectivity for the sorption of anionic compounds in aqueous solution.

Table 1: Elemental microanalysis data of poly(AN-*co*-DVB-80-*co*-VBC) and hypercrosslinked poly(AN-*co*-DVB-80-*co*-VBC) terpolymers before and after chemical modification

Sample	Mole fraction of AN/DVB-80/VBC, %	Elemental microanalysis, %			
		C	H	N	Cl
P1	35/60/5	81.3	7.1	3.8	1.0
HXL P1		79.9	6.7	3.1	0.6
EDA-HXL P1		65.1	7.5	20	0.6

3.4 Scanning electron microscopy analysis

The SEM images and the polynomial distribution of all terpolymer samples, namely P1, HXL P1, and EDA-HXL P1 are presented in Figure 3a–f. As shown in Figure 3a, the terpolymer particles of P1 are in the form of spherical polymer microspheres, and the morphologies of the polymers (Figure 3c) are still retained through the hypercrosslinking reactions. As shown in Figure 3e, EDA-modified HXL terpolymer particles are still in the form of spherical beads.

The polynomial distribution of spherical porous terpolymer particles was determined by calculating the mean diameter and standard deviation of particles based on the measurement of 100 particle diameters from SEM images

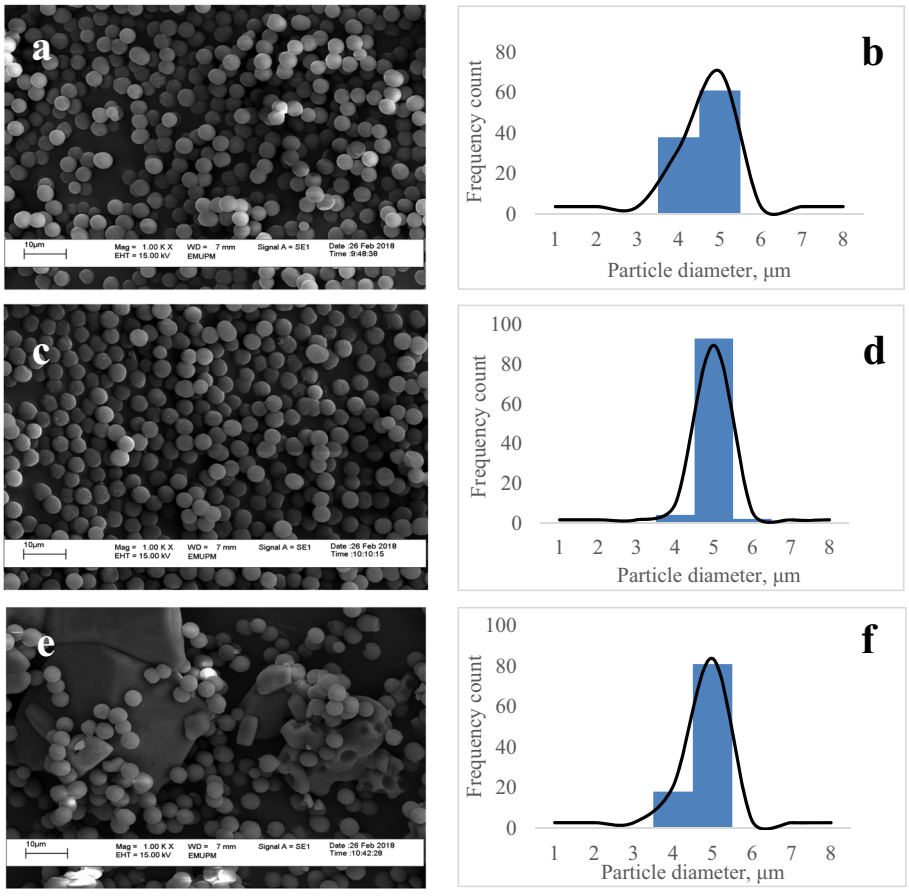

Figure 3: SEM images and polynomial distribution: (a) SEM image of P1, (b) polynomial distribution of P1, (c) SEM image of HXL P1, (d) polynomial distribution of HXL P1, (e) SEM image of EDA-HXL P1, and (f) polynomial distribution of EDA-HXL P1.

(by using the ImageJ software). The results showed that the maximum frequency count was obtained at 5 µm of the particle diameter for P1 (Figure 3b), HXL P1 (Figure 3d), and EDA-HXL P1 (Figure 3f).

As presented in Table 2, the mean particle diameter of the poly(AN-*co*-DVB-80-*co*-VBC) (P1), hypercrosslinked poly (AN-*co*-DVB-80-*co*-VBC) (HXL P1), and EDA-modified hypercrosslinked poly(AN-*co*-DVB-80-*co*-VBC) (EDA-HXL P1) was similar to one another, at ~4.0 µm, even after the chemical modification was carried out. The C_v values indicated that all poly(AN-*co*-DVB-80-*co*-VBC), HXL poly (AN-*co*-DVB-80-*co*-VBC), and EDA-modified HXL poly(AN-*co*-DVB-80-*co*-VBC) were quasi-monodisperse (C_v value between 5% and 15%) (32).

3.5 Brunauer–Emmett–Teller surface area analysis

The porosity of the polymers isolated from the precipitation polymerisation and its chemically modified hypercrosslinked variants was determined using nitrogen sorption analysis and the application of the Brunauer–Emmett–Teller (BET) theory. Table 3 presents the nitrogen sorption analysis data obtained for poly(AN-*co*-DVB-80-*co*-VBC), hypercrosslinked poly(AN-*co*-DVB-80-*co*-VBC), and EDA-modified HXL poly(AN-*co*-DVB-80-*co*-VBC).

As presented in Table 3 and as expected, the BET-specific surface area increased significantly from 471 $m^2\ g^{-1}$ (P1) to 983 $m^2\ g^{-1}$ (HXL P1), upon the hypercrosslinking reaction. The specific pore volume was also increased in the range of 0.327–0.731 $cm^3\ g^{-1}$. However, after the chemical modification with EDA, the BET-specific surface area decreased to 503 $m^2\ g^{-1}$, while the mean pore size increased to 4.7 nm. Fontanals et al. carried out a chemical modification toward poly(DVB-80-VBC) copolymer, in which the post-hypercrosslinking chemical modification (by using ethylenediamine and piperazine) occurred on residual chloromethyl groups from the VBC units in the copolymer. As a consequence, the porosity of the chemically modified copolymers was retained throughout the chemical modification process (25). Cormack et al. performed post-

Table 2: The particle size of poly(AN-*co*-DVB-80-*co*-VBC) and hypercrosslinked poly(AN-*co*-DVB-80-*co*-VBC) terpolymers before and after the chemical modification

Sample	AN/DVB-80/VBC, mol%	Mean particle diameter, μm	Coefficient of variation, %	Dispersity
P1	35/60/5	4.1	6	Quasi-monodisperse
HXL P1		4.4	6	Quasi-monodisperse
EDA-HXL P1		4.2	6	Quasi-monodisperse

Table 3: BET data of poly(AN-*co*-DVB-80-*co*-VBC) and hypercrosslinked poly(AN-*co*-DVB-80-*co*-VBC) terpolymers before and after the chemical modification with EDA

Sample	AN/DVB-80/VBC, mol%	Specific surface area, m^2/g	Specific pore volume, cm^3/g	Mean pore size, nm
P1	35/60/5	471	0.327	2.7
HXL P1		983	0.731	3.0
EDA-HXL P1		503	2.664	4.7

polymerisation chemical modification of poly(DVB-80-*co*-VBC) with lauryl sulfate. The sulphonate group was developed within the benzene ring of the methylene bridge (upon hypercrosslinking reaction). It was reported that the lauryl sulphate-modified HXL copolymer displayed high specific surface areas (1,370 $m^2 g^{-1}$) (26). In the present study, the idea was to chemically modify the terpolymer system by consuming nitrile groups from the AN unit in the terpolymer and converting the nitrile into diamine (by using ethylenediamine) moieties. The confirmation of the chemical modifications on nitrile moieties was proved by the FT-IR spectra in Figure 1c. In contrast to what has been achieved by Fontanals et al. and Cormack et al., this study showed that chemical modifications toward nitrile moieties with amine-based reagent caused the disruption of specific surface areas and enlargement of mean pore size. This might be due to the disruption of the walls within the hypercrosslinked terpolymer system as the AN unit was chemically modified. A similar observation was reported by Andhi et al., in which the residual chloromethyl groups from the VBC units in the AN/DVB/VBC terpolymer that had functionalised with ethylenediamine displayed a very low specific surface area (0.07 $m^2 g^{-1}$) (33).

3.6 Drugs adsorption – application of poly (AN-*co*-DVB-80-*co*-VBC), HXL poly(AN-*co*-DVB-80-*co*-VBC), and EDA-modified HXL poly(AN-*co*-DVB-80-*co*-VBC)

The adsorption ability of poly(AN-*co*-DVB-80-*co*-VBC), HXL poly(AN-*co*-DVB-80-*co*-VBC), and EDA-modified HXL poly(AN-*co*-DVB-80-*co*-VBC) to adsorb acidic pharmaceuticals which included diclofenac (DCF), mefenamic acid (MA), and metronidazole (MNZ) was studied in the batch system. The percentage removal of pharmaceuticals by poly(AN-*co*-DVB-80-*co*-VBC) (at varied contact time) is the lowest as observed from Table 4. As expected from the BET surface area analysis, the HXL poly(AN-*co*-DVB-80-*co*-VBC) with the highest surface area achieved the highest percentage removal of drugs (DCF, 87%; MA, 85%; MNZ, 87%).

After the modification with ethylenediamine, the EDA-modified HXL poly(AN-*co*-DVB-80-*co*-VBC) possessed more positively charged species due to the present of pendant diamine groups on the terpolymer surface, which enhanced the selectivity toward the polar analytes (34). The adsorption capacity was increased significantly by 38%, 36%, and 20% for the sorption of DCF, MA and MNZ, respectively compared with the adsorption capacity of the unmodified hypercrosslinked sample. Henceforth, the modified HXL poly(AN-*co*-DVB-80-*co*-VBC) and HXL poly(AN-*co*-DVB-80-*co*-VBC) adsorbents were selected as a detailed study for the adsorption of acidic pharmaceuticals.

3.7 Adsorption isotherms

The equilibrium adsorption studies were carried out to describe the relationship between adsorbate and adsorbent molecules. The adsorption mechanism could be analysed by comparing the best fitting adsorption isotherm models with the equilibrium data obtained.

Table 4: Adsorption test of pharmaceuticals on P1, HXL P1, and EDA-HXL P1 terpolymers with variation of times

Adsorbent	Time (min)	Diclofenac (DCF)		Mefenamic acid (MA)		Metronidazole (MNZ)	
		Percentage removal (%)	Improvement (%)	Percentage removal (%)	Improvement (%)	Percentage removal (%)	Improvement (%)
P1	2	43.96	—	45.71	—	54.90	—
	4	44.10	—	46.19	—	55.60	—
	6	44.47	—	46.85	—	54.88	—
	8	46.35	—	48.02	—	57.12	—
	10	44.98	—	46.41		58.48	
HXL P1	2	79.94	35.98	82.29	36.58	81.86	26.96
	4	79.36	35.26	81.09	34.90	81.47	25.87
	6	80.05	35.58	81.69	34.84	80.73	25.85
	8	87.01	40.66	84.91	36.89	87.31	30.19
	10	86.83	41.85	81.18	34.77	81.60	23.12
EDA-HXL P1	2	77.71	33.75	81.64	35.93	81.84	26.94
	4	78.17	34.07	82.04	35.85	78.76	23.16
	6	77.38	32.91	81.23	34.38	78.57	23.69
	8	82.48	36.13	84.28	36.26	83.35	26.23
	10	82.99	38.01	81.92	35.51	78.91	20.43

Default pH; initial concentration, C_o: 20 mg L^{-1}; adsorbent dosage: 10 mg; centrifugation speed: 4,000 rpm.

The significance of the isotherm study is to delineate the adsorption behaviour of diclofenac (DCF), mefenamic acid (MA), and metronidazole (MNZ) onto the surface of HXL P1 and EDA-HXL P1 terpolymers. Two isotherm models were selected in this present study: Langmuir and Freundlich isotherms. The linearised form of the Langmuir and Freundlich models can be expressed as Eq. 4 and 5, respectively (35):

$$\frac{1}{q_e} = \frac{1}{C_e}\frac{1}{K_L . q_m} + \frac{1}{q_m} \quad (4)$$

$$\log q_e = \frac{1}{n}\log C_e + \log K_F \quad (5)$$

where K_L is the Langmuir constant (L mg^{-1}), q_m is the maximum amount of drugs adsorbed (mg g^{-1}), C_e is the equilibrium concentration of acidic drugs (mg L^{-1}), and q_e is the amount of acidic drugs adsorbed at the equilibrium (mg g^{-1}). K_F represents the Freundlich constant [(mg/g) $(L\ mg^{-1})^{1/n}$], and n is the heterogeneity factor. For the Langmuir model, q_m can be calculated from the intercept, and K_L could be deduced from the gradient. In the case of Freundlich isotherm, n and K_F could be calculated, respectively, from the slope and intercept.

The calculated values of the isotherm parameters such as q_m, K_L, K_F, and n, as well as regression coefficients (R^2) are summarized in Table 5 (Appendix Figures A1 and A2 represent the Langmuir and Freundlich plot isotherms, respectively).

Based on the R^2 values (>0.98), both Langmuir and Freundlich models were found to be suitable for the description of equilibrium adsorption data. This indicated the possibility of both monolayer and multilayer adsorption systems. The calculated maximum adsorption capacity of the HXL P1 adsorbent by the Langmuir equation for DCF, MA, and MNZ was 526, 1,667, and 1,667 mg g^{-1}, respectively, while

Table 5: Isotherm parameters of drugs adsorption by HXL P1 and EDA-HXL P1 terpolymers

Adsorbent	Drugs	Langmuir			Freundlich		
		q_m (mg/g)	K_L (L/mg)	R^2	K_F [(mg/g) $(L/mg)^{1/n}$]	n	R^2
HXL P1	DCF	526.32	2.39×10^{-3}	0.9870	3.49	0.87	0.9974
	MA	1666.67	9.59×10^{-4}	0.9996	2.14	0.94	1.0000
	MNZ	1666.67	9.77×10^{-4}	0.9999	1.92	0.94	0.9999
EDA-HXL P1	DCF	434.78	2.73×10^{-3}	0.9826	2.70	0.86	0.9964
	MA	2000.00	8.07×10^{-4}	0.9999	2.12	0.94	0.9998
	MNZ	2500.00	6.76×10^{-4}	0.9999	1.87	0.95	0.9998

Table 6: Kinetic parameters for the adsorption of drugs onto HXL P1 and EDA-HXL P1 terpolymers

Kinetic models	Parameters	HXL P1			EDA-HXL P1		
		DCF	MA	MNZ	DCF	MA	MNZ
Pseudo-first-order	k_1 (min^{-1})	0.52	0.32	0.32	0.42	0.31	0.26
	$q_{e(exp)}$ (mg/g)	35.00	34.00	35.00	33.40	33.90	33.50
	$q_{e(cal)}$ (mg/g)	0.31	0.13	0.05	0.17	0.14	0.17
	R^2	0.7979	0.4158	0.4259	0.7563	0.4878	0.3461
Pseudo-second-order	k_2 (g/mg min)	0.061	2.33	1.95	0.093	0.88	0.50
	$q_{e(exp)}$ (mg/g)	35.00	34.00	35.00	33.40	33.90	33.50
	$q_{e(cal)}$ (mg/g)	35.97	32.97	32.05	33.90	33.11	33.44
	R^2	0.9957	0.9977	0.9967	0.9976	0.9989	0.9945

the EDA-HXL P1 maximum sorption capacity was 435 mg g^{-1} (DCF), 2,000 mg g^{-1} (MA), and 2,500 mg g^{-1} (MNZ), respectively. The EDA-HXL P1 terpolymer exhibited higher adsorption performance toward MA and MNZ, compared to HXL P1. Conversely, HXL P1 terpolymer showed better adsorption capacity toward DCF (36). This observation can be explained by the fact that the EDA-HXL P1 terpolymer developed new diamine functional groups in its structure, which might have enhanced the selectivity, despite its lower specific surface area (503 m^2 g^{-1}) compared to HXL P1 terpolymer (983 m^2 g^{-1}).

The adsorption is linear if the n value is equal to unity; chemisorption is more favourable if $n < 1$; physiosorption is more favourable if $n > 1$ (37). Table 5 reveals that all drugs have an n value less than 1, for both HXL P1 and EDA-HXL P1 terpolymers; thus, the adsorption of DCF, MA, and MNZ was more likely to be a chemisorption process.

3.8 Adsorption kinetics

The kinetic study of the adsorption process was evaluated to determine the adsorption behaviour such as the adsorption mechanism, the rate of reaction, and the change in adsorption capacity within a certain time (37). The experimental data for the adsorption of pharmaceuticals (DCF, MA, and MNZ) onto HXL P1 and EDA-HXL P1 terpolymers were analysed using two kinetic models, the pseudo-first-order and pseudo-second-order models. The Lagergren pseudo-first-order and pseudo-second-order kinetic models can be described linearly as Eq. 6 and 7, respectively (38,39):

$$\log(q_e - q_t) = \log q_e - \frac{k_1}{2.303}t \quad (6)$$

$$\frac{t}{q_t} = \frac{1}{k_2 q_e^2} + \frac{1}{q_e}t \quad (7)$$

where q_e and q_t are the amount of drugs adsorbed on the surface of the sorbent (mg g^{-1}) at equilibrium and at time, t (min), respectively; k_1 and k_2 are the pseudo-first-order rate constant (min^{-1}) and pseudo-second-order constant (g/mg min).

Table 6 presents the adsorption kinetic parameters of the adsorbates. The application of pseudo-first-order and pseudo-second-order models for the kinetic data of DCF, MA, and MNZ was presented in Appendix Figures A3 and A4, respectively.

It was noticeable that the pseudo-first-order model did not fit well with the experimental data. This is proven by the correlation coefficient (R^2) values, which were low for both HXL P1 (0.4158-0.7979) and EDA-HXL P1 (0.3461-0.7563). Besides, the predicted adsorption capacity values ($q_{e(cal)}$) by pseudo-first-order model varied significantly from its corresponding experimental value at equilibrium ($q_{e(exp)}$). On the contrary, the correlation coefficient (R^2) values for both polymers and all drugs adsorbed were greater than 0.99, which clearly indicated that the pseudo-second-order rate model better represented the experimental data than the pseudo-first-order kinetic model. In addition, the equilibrium adsorption capacity $q_{e(exp)}$ had better agreement with the calculated values $q_{e(cal)}$. This confirmed that the pseudo-second-order model was preferred and was more suitable for the description of adsorption kinetic. Therefore, the uptake of DCF, MA, and MNZ onto both terpolymers was chemisorption in nature. These results agreed with other studies, which found that the pseudo-second-order kinetic model was perfectly applicable for the adsorption of ibuprofen by immobilised polymeric adsorbent (40). Oleszczuk also reported that the kinetics of diclofenac and naproxen favoured mainly

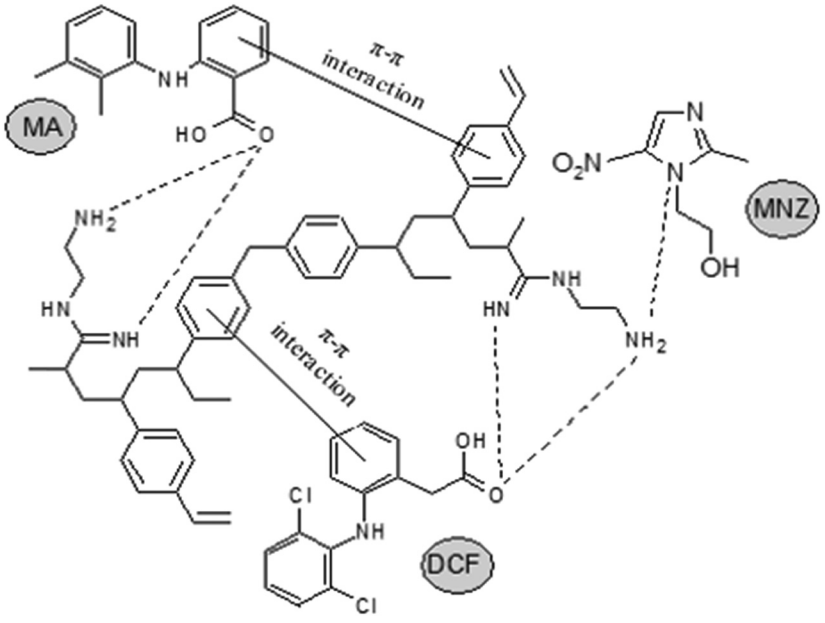

Figure 4: Proposed interaction mechanism of DCF (diclofenac), MA (mefenamic acid), and MNZ (metronidazole) toward the active sites of EDA-modified HXL poly(AN-*co*-DVB-80-*co*-VBC).

the pseudo-second-order model onto carbon nanotubes (CNTs) treated by UV/H_2O_2 (41).

3.9 Proposed interaction mechanism between EDA-HXL P1 with pharmaceuticals

The possible adsorption mechanism of reaction between EDA-modified HXL poly(AN-*co*-DVB-80-*co*-VBC) and acidic pharmaceuticals is shown in Figure 4. It was found that EDA-HXL P1 terpolymer had a better performance in adsorbing the pharmaceuticals as proved by the maximum adsorption capacity (q_m) values in which the drugs uptake increased up to 96% (2,000 mg g^{-1} of adsorption capacity). The EDA-HXL P1 terpolymer demonstrated a better adsorptive performance due to the presence of active sites on the adsorbent surface. The polar diamine functional group ($-NH_2$ and =N–H) in the EDA-modified HXL poly(AN-*co*-DVB-80-*co*-VBC) interacted with the polar molecules of the analytes via hydrogen bonding and electrostatic interaction (H–O and H–N), which attributed to the strong interactions between active sites in the EDA-HXL P1 with the polar acidic compounds. The existence of strong π–π interactions between adsorbates and EDA-HXL P1 were also expected since EDA-HXL P1 possessed a polar diamine functional group (electron-donating) on their benzene ring. EDA-HXL P1 had better interaction with acidic pharmaceuticals despite its lower specific surface area compared to the HXL P1.

4 Conclusion

Poly(AN-*co*-DVB-80-*co*-VBC) terpolymers were synthesised and hypercrosslinked with $FeCl_3$ via precipitation polymerisation and Friedel–Crafts reaction, respectively. A functional hypercrosslinked polymer was successfully prepared by a chemically modified HXL poly(AN-*co*-DVB-80-*co*-VBC) with ethylenediamine. The surface morphology of diamine-modified HXL poly(AN-*co*-DVB-80-*co*-VBC) showed spherical beads with monodisperse microspheres particles of ~4.0 µm. The monodispersity of the particles showed that the particles had a potential for application in the SPE system. Both HXL poly(AN-*co*-DVB-80-*co*-VBC) and diamine-modified HXL poly(AN-*co*-DVB-80-*co*-VBC) had specific surface areas of 983 $m^2 g^{-1}$ and 503 $m^2 g^{-1}$, respectively. The diamine-modified HXL poly(AN-*co*-DVB-80-*co*-VBC) exhibited high adsorption capacity for acidic drugs, which was mainly due to strong ion-exchange interactions between positively charged diamine functional groups and anionic polar compounds. The adsorption behaviour of DCF, MA, and MNZ onto HXL poly(AN-*co*-DVB-80-*co*-VBC) and diamine-modified HXL poly(AN-*co*-DVB-80-*co*-VBC) terpolymers satisfied the

Langmuir and Freundlich isotherms. The kinetic model of the pseudo-second order (R^2 = 0.999) was the best model for describing the adsorption rate of all drugs (DCF, MA, and MNZ). Both hypercrosslinked and chemically modified hypercrosslinked poly(AN-*co*-DVB-80-*co*-VBC) showed an excellent adsorption performance with high capacity and selectivity for the removal of acidic pharmaceuticals.

Acknowledgments: The authors would like to acknowledge the Chemistry Department of the Faculty of Science in Universiti Putra Malaysia (UPM), Department of Chemical and Environmental Engineering, Faculty of Engineering in Universiti Putra Malaysia (UPM), and WestCHEM of the Department of Pure and Applied Chemistry in the University of Strathclyde in the UK. The authors would also like to express gratitude to the Ministry of Higher Education Malaysia for the financial support given via the Fundamental Research Grant Scheme, project code FRGS/1/2013/SG01/UPM/02/3 (02-01-13-1215FR).

Conflicts of interest: The authors declare that they have no conflict of interest.

References

(1) McEneff G, Barron L, Kelleher B, Paull B, Quinn B. A year-long study of the spatial occurrence and relative distribution of pharmaceutical residues in sewage effluent, receiving marine waters and marine bivalves. Sci Total Environ. 2014;476:317–26.
(2) Tewari S, Jindal R, Kho YL, Eo S, Choi K. Major pharmaceutical residues in wastewater treatment plants and receiving waters in Bangkok, Thailand, and associated ecological risks. Chemosphere. 2013;91:697–704.
(3) Hughes SR, Kay P, Brown LE. A global synthesis and critical evaluation of pharmaceutical datasets collected from river systems. Environ Sci Technol. 2012;47(2):661–77.
(4) Jones OA, Lester JN, Voulvoulis N. Pharmaceuticals: a threat to drinking water? Trends Biotechnol. 2005;23(4):163–7.
(5) Al-Qaim FF, Abdullah MP, Othman MR, Latip J, Zakaria Z. Multi-residue analytical methodology-based liquid chromatography-time-of-flight-mass spectrometry for the analysis of pharmaceutical residues in surface water and effluents from sewage treatment plants and hospitals. J Chromatogr A. 2014;1345:139–53.
(6) Praveena SM, Shaifuddin SNM, Sukiman S, Nasir FAM, Hanafi Z, Kamarudin N, et al. Pharmaceuticals residues in selected tropical surface water bodies from Selangor (Malaysia): occurrence and potential risk assessments. Sci Total Environ. 2018;642:230–240.
(7) Yacob H, Ling YE, Hee-young K, Zainura O, Noor Z, Fadhil M, et al. Identification of pharmaceutical residues in treated sewage effluents in Johor, Malaysia. Malaysian J Civil Eng. 2017;29:165–173.
(8) Lonappan L, Kaur S, Kumar R, Verma M, Surampalli RY. Diclofenac and its transformation products: environmental occurrence and toxicity – a review. Environ Int. 2016;96:127–138.
(9) Bonne B, Gomez E, Courant F, Escande A, Fenet H. Diclofenac in the marine environment: a review of its occurrence and effects. Marine Pollut Bull. 2018;131:496–506.
(10) Manjunath SV, Kumar SM, Ngo HH, Guo W. Toxic/Hazardous Substances and Environmental Engineering Metronidazole removal in powder-activated carbon and concrete-containing graphene adsorption systems: estimation of kinetic, equilibrium and thermodynamic parameters and optimization of adsorpti. J Environ Sci Health Part A. 2017;52(14):1269–83.
(11) Zhang X, Li G, Zhang H, Wang X, Qu J, Liu P, et al. Enhanced adsorption capacity and selectivity towards salicylic acid in water by a cationic polymer. Soft Matter. 2013;9(26):6159–66.
(12) Buszewski B, Szultka M. Past, present, and future of solid phase extraction: a review. Crit Rev Anal Chem. 2012;42:198–213.
(13) Bratkowska D, Fontanals N, Borrull F, Cormack PAG, Sherrington DC, Marcé RM. Hydrophilic hypercrosslinked polymeric sorbents for the solid-phase extraction of polar contaminants from water. J Chromatogr A. 2010;1217:3238–3243.
(14) Chen J, Zhao C, Huang H, Wang M, Ge X. Highly crosslinked poly(ethyleneglycol dimethacrylate)-based microspheres via solvothermal precipitation polymerization in alcohol–water system. Polymer. 2016;83:214–222.
(15) Ling X, Li H, Zha H, He C, Huang J. Polar-modified post-cross-linked polystyrene and its adsorption towards salicylic acid from aqueous solution. Chem Eng J. 2016;286:400–407.
(16) Fontanals N, Marc RM, Borrull F, Cormack PAG. Hypercrosslinked materials: Preparation, characterisation and applications. Polym Chem. 2015;6:7231–7244.
(17) Huang J, Wang G, Huang K. Enhanced adsorption of salicylic acid onto a β-naphthol-modified hyper-cross-linked poly (styrene-*co*-divinylbenzene) resin from aqueous solution. Chem Eng J. 2011;168:715–721.
(18) Fontanals N, Marcé RM, Borrull F. New materials in sorptive extraction techniques for polar compounds. J Chromatogr A. 2007;1152(1–2):14–31.
(19) Nida N, Subri S, Cormack PAG, Nurul S, Jamil A, Abdullah LC, et al. Synthesis of poly(acrylonitrile-*co*-divinylbenzene-*co*-vinylbenzyl chloride)-derived hypercrosslinked polymer microspheres and a preliminary evaluation of their potential for the solid-phase capture of pharmaceuticals. J Appl Polym Sci. 2018;45677:1–9.
(20) Huang H, Ding Y, Chen X, Chen Z, Kong XZ. Synthesis of monodisperse micron-sized poly(divinylbenzene) microspheres by solvothermal precipitation polymerization. Chem Eng J. 2016;289:135–141.
(21) Jalilian R, Taheri A. Synthesis and application of a novel core–shell–shell magnetic ion imprinted polymer as a selective adsorbent of trace amounts of silver ions. E-Polymers. 2018;18:123–134.

(22) Khoddami N, Shemirani F. A new magnetic ion-imprinted polymer as a highly selective sorbent for determination of cobalt in biological and environmental samples. Talanta. 2016;146:244–52.
(23) Behbahani M, Bagheri A, Taghizadeh M, Salarian M, Sadeghi O, Adlnasab L, et al. Synthesis and characterisation of nano structure lead(II) ion-imprinted polymer as a new sorbent for selective extraction and preconcentration of ultra trace amounts of lead ions from vegetables, rice, and fish samples. Food Chem. 2013;138:2050–2056.
(24) Kuang W, Liu YN, Huang J. Phenol-modified hyper-cross-linked resins with almost all micro/mesopores and their adsorption to aniline. J Colloid Interface Sci. 2017;487:31–37.
(25) Fontanals N, Cormack PAG, Sherrington DC. Hypercrosslinked polymer microspheres with weak anion-exchange character. Preparation of the microspheres and their applications in pH-tuneable, selective extractions of analytes from complex environmental samples. J Chromatogr A. 2008;1215:21–29.
(26) Cormack PAG, Davies A, Fontanals N. Synthesis and characterization of microporous polymer microspheres with strong cation-exchange character. React Funct Polym. 2012;72:939–946.
(27) Fontanals N, Marc RM, Borrull F, Cormack PAG. Hypercrosslinked materials: preparation, characterisation and applications. Polym Chem. 2015;6:7231–7244.
(28) Bratkowska D, Davies A, Fontanals N, Cormack PAG, Borrull F, Sherrington DC, et al. Hypercrosslinked strong anion-exchange resin for extraction of acidic pharmaceuticals from environmental water. J Sep Sci. 2012;35:2621–2628.
(29) Subri NNS, Cormack PAG, Jamil Md, Abdullah SNA, Daik LC, R. Synthesis of poly(acrylonitrile-*co*-divinylbenzene-*co*-vinylbenzyl chloride)-derived hypercrosslinked polymer microspheres and a preliminary evaluation of their potential for the solid-phase capture of pharmaceuticals. J Appl Polym Sci. 2018;135:45677.
(30) Fontanals N, Marcé RM, Borrull F, Cormack PAG. Mixed-mode ion-exchange polymeric sorbents: dual-phase materials that improve selectivity and capacity. TrAC Trends Anal Chem. 2010;29:765–779.
(31) Cai N, Larese-Casanova P. Application of positively-charged ethylenediamine-functionalized graphene for the sorption of anionic organic contaminants from water. J Environ Chem Eng. 2016;4:2941–2951.
(32) Gokmen MT, Du Prez FE. Porous polymer particles – a comprehensive guide to synthesis, characterization, functionalization and applications. Progr Polym Sci. 2012;37:365–405.
(33) Andhi MRG, Eenakshi SM, Amada MY. Preparation of amino functionalized polymeric resins for selective removal of copper ions. Int J Soc Mater Eng Resour. 2014;20:71–76.
(34) Adeyi AA, Jamil SNAM, Abdullah LC, Choong TSY. Adsorption of malachite green dye from liquid phase using hydrophilic thiourea-modified poly(acrylonitrile-*co*-acrylic acid): kinetic and isotherm studies. J Chem. 2019;2019:14.
(35) Ebrahimi R, Hayati B, Shahmoradi B, Rezaee R, Safari M, Maleki A, et al. Adsorptive removal of nickel and lead ions from aqueous solutions by poly(amidoamine) (PAMAM) dendrimers ([formula presented]). Environ Technol Innov. 2018;12:261–272.
(36) Frankowski M, Popenda Ł. A new low-cost polymeric adsorbents with polyamine chelating groups for efficient removal of heavy metal ions from water solutions. React and Funct Polym. 2018;131:64–74.
(37) Amirah N, Zahri M, Nurul S, Jamil A, Chuah L, Jia S, et al. Equilibrium and kinetic behavior on cadmium and lead removal by using synthetic polymer. J Water Proc Eng. 2017;17:277–289.
(38) Ho YS. Second-order kinetic model for the sorption of cadmium onto tree fern: a comparison of linear and non-linear methods. Water Res. 2006;40:119–125.
(39) Nimibofa A, Augustus EN. Comparative sorption studies of dyes and metal ions by Ni/Al-layered double hydroxide. Int J Mater Chem. 2017;7:25–35.
(40) Shang S, Chiu K, Jiang S. Synthesis of immobilized poly(vinyl alcohol)/cyclodextrin eco-adsorbent and its application for the removal of ibuprofen from pharmaceutical sewage. J Appl Polym Sci. 2017;44861:1–7.
(41) Oleszczuk P. Sorption of diclofenac and naproxen onto MWCNT in model wastewater treated by H_2O_2 and/or UV. Chemosphere. 2016;149:272–8.

Appendix

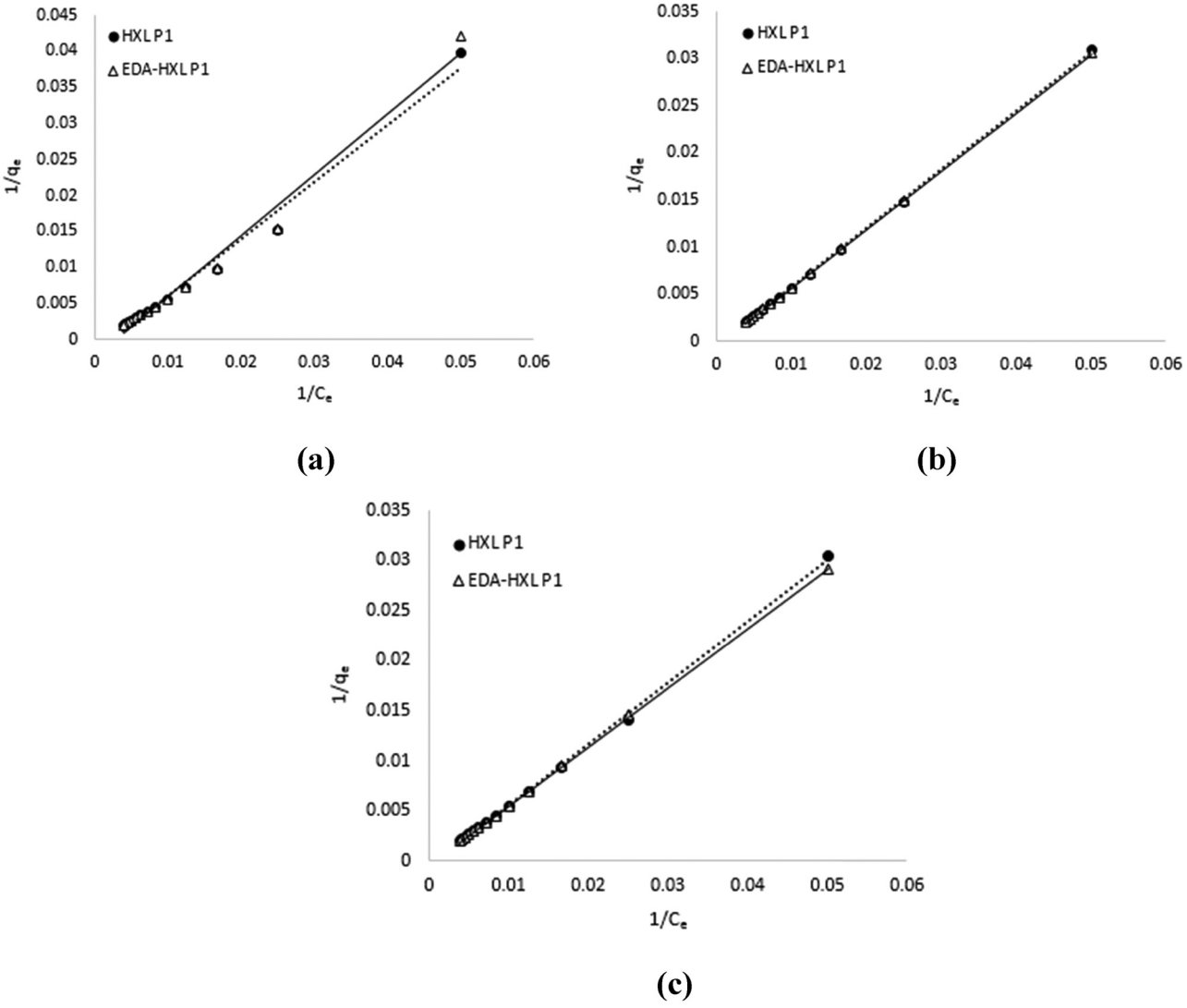

Figure A1: Langmuir plots for the pharmaceuticals adsorption of (a) DCF, (b) MA, and (c) MNZ by HXL PI and EDA-HXL P1 terpolymers.

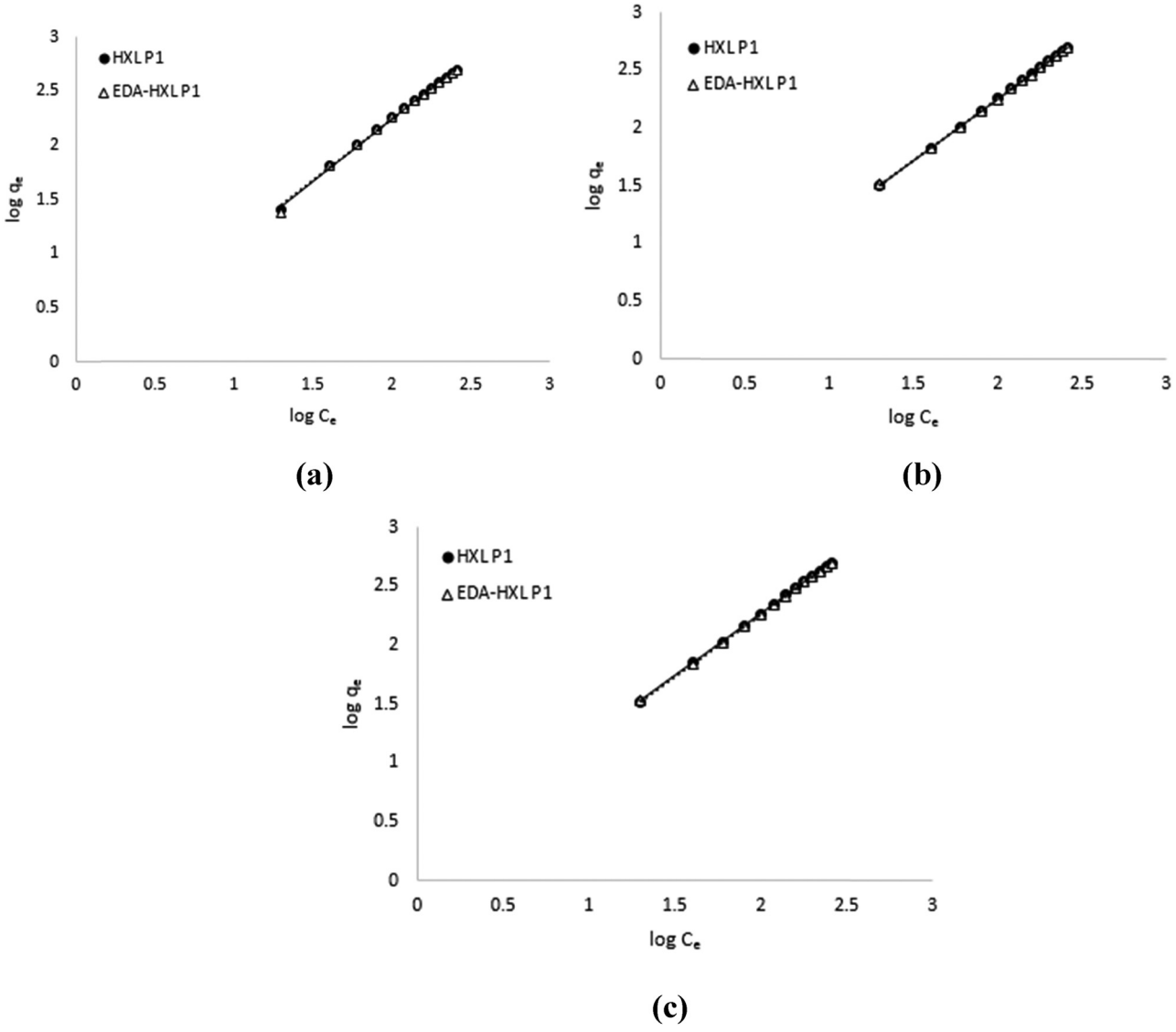

Figure A2: Freundlich isotherm plots for the pharmaceuticals adsorption of (a) DCF, (b) MA, and (c) MNZ by HXL PI and EDA-HXL P1 terpolymers.

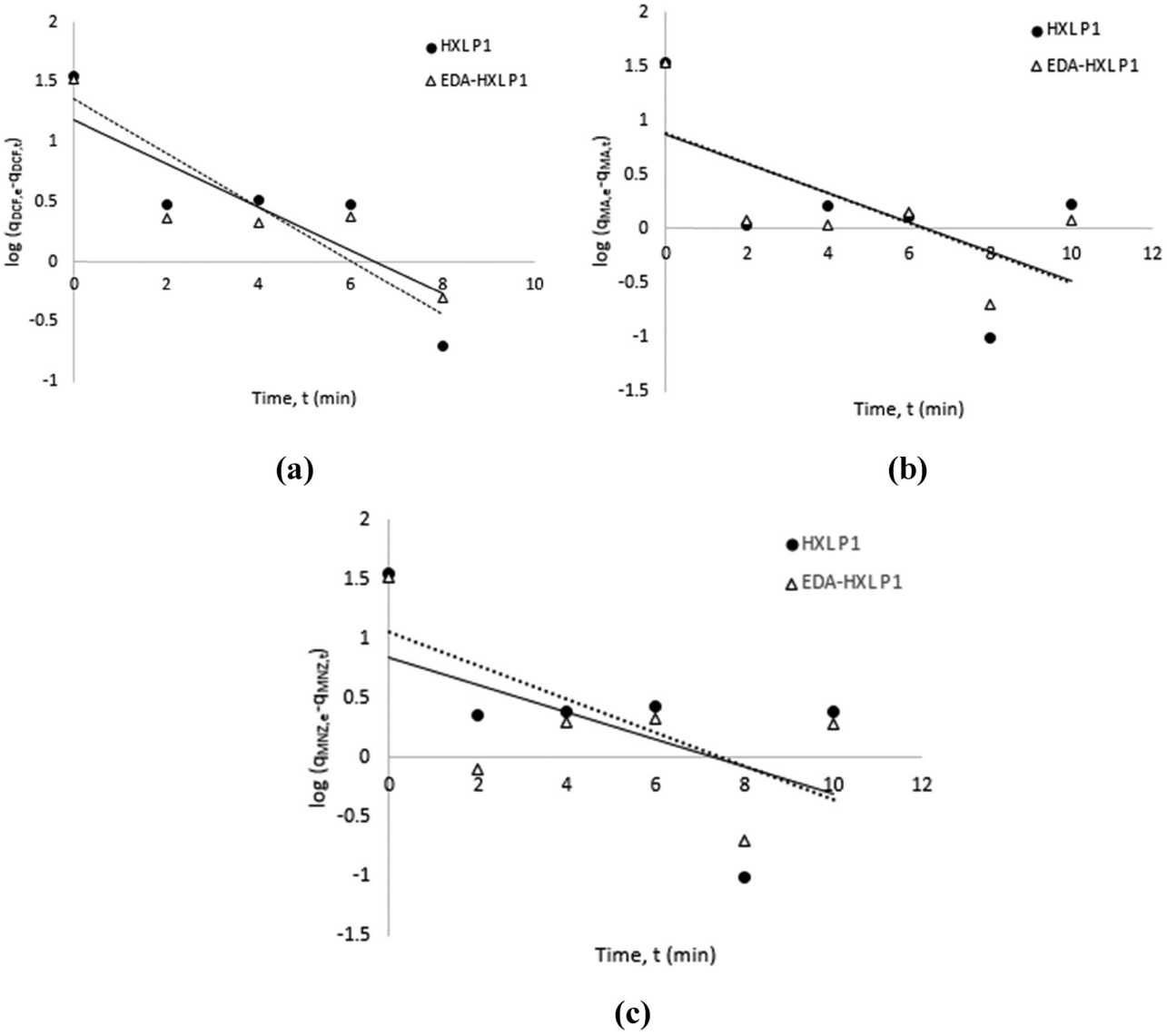

Figure A3: Pseudo-first-order kinetic model for the adsorption of (a) DCF, (b) MA, and (c) MNZ by HXL PI and EDA-HXL P1 terpolymers.

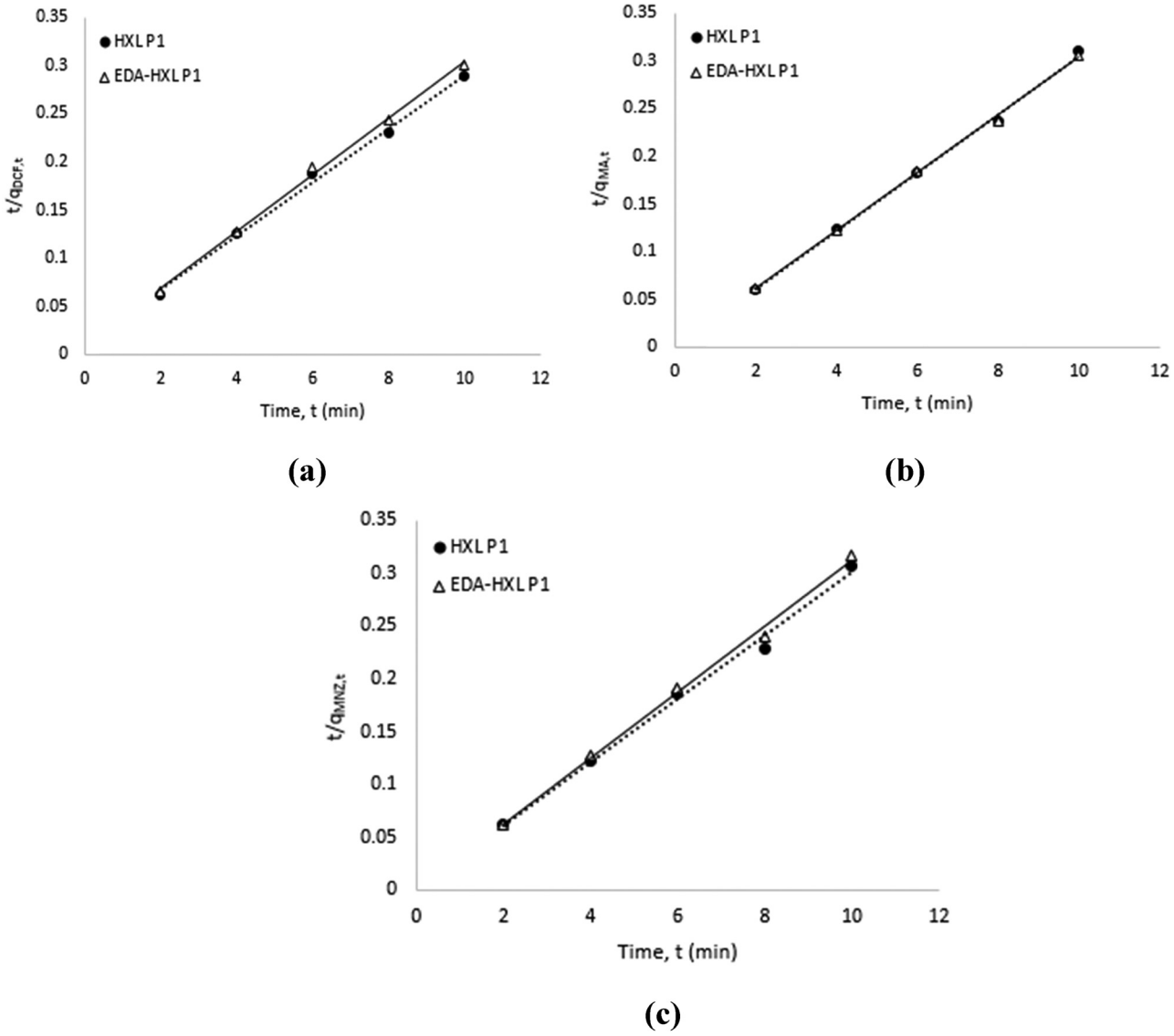

Figure A4: Pseudo-second-order kinetic model for the adsorption of (a) DCF, (b) MA, and (c) MNZ by HXL PI and EDA-HXL P1 terpolymers.